Published for SISSA by Springer

Received: July 7, 2017
Revised: August 16, 2017
Accepted: October 16, 2017
Published: November 6, 2017

A neutrinophilic 2HDM as a UV completion for the inverse seesaw mechanism

Enrico Bertuzzo,[a] **Pedro A.N. Machado,**[b] **Zahra Tabrizi**[a] **and Renata Zukanovich Funchal**[a]

[a] *Departamento de Física Matemática, Instituto de Física, Universidade de São Paulo, C.P. 66.318, São Paulo, 05315-970 Brazil*

[b] *Departamento de Física Matemática, Instituto de Física, Universidade de São Paulo, R. do Matão, 1371, Butantã, São Paulo, SP, 05508-090 Brazil*

E-mail: bertuzzo@if.usp.br, pmachado@fnal.gov, ztabrizi@if.usp.br, zukanov@if.usp.br

Abstract: In Neutrinophilic Two Higgs Doublet Models, Dirac neutrino masses are obtained by forbidding a Majorana mass term for the right-handed neutrinos via a symmetry. We study a variation of such models in which that symmetry is taken to be a local U(1), leading naturally to the typical Lagrangian of the inverse seesaw scenario. The presence of a new gauge boson and of an extended scalar sector result in a rich phenomenology, including modifications to Z, Higgs and kaon decays as well as to electroweak precision parameters, and a pseudoscalar associated to the breaking of lepton number.

Keywords: Beyond Standard Model, Higgs Physics, Neutrino Physics

ArXiv ePrint: 1706.10000

https://doi.org/10.1007/JHEP11(2017)004

JHEP11(2017)004

Contents

JHEP11(2017)004

1 Introduction

More than two decades of neutrino experiments have confirmed that neutrinos are massive particles and oscillate. Strong bounds from cosmological [1] and terrestrial [2] experiments suggest that neutrino masses should be below the eV scale. This may be an indication that the mechanism behind the generation of neutrino masses may be different from the Higgs mechanism of the Standard Model (SM).

The seesaw mechanism is one of the most elegant and economic ways to explain the smallness of neutrino masses [3–5]. In the Type-I seesaw, the SM particle content is enlarged by at least two heavy right-handed neutrino singlets, N_i (i denotes the generation), such that the neutrino mass generation mechanism reads

$$-\mathcal{L}_\nu = y^\nu_{ij}\,\bar{\ell}_{iL}\tilde{H}N_j + \frac{1}{2}M^i_R\overline{N^c_i}N_i + \text{h.c.}\,, \tag{1.1}$$

where ℓ_{iL} are the SM lepton doublets, H is the SM Higgs scalar doublet and the tilde denotes charge conjugation. The heavy neutrino mass scale suppresses the Dirac mass term contribution typically resulting in active neutrino masses $m_\nu \simeq -v^2 y^{\nu\,T} {M_R}^{-1} y^\nu$, where $v = 246\,\text{GeV}$ is the electroweak (EW) scale. To avoid tiny Yukawa couplings (of order 10^{-11} or so) and still have neutrino masses in the sub-eV range, the right-handed neutrinos should be at a very high scale, $\mathcal{O}(10^{13})\,\text{GeV}$, which makes the model generally inaccessible to experiments except perhaps to future neutrinoless double beta decay measurements. This remains true even if the right-handed neutrinos are taken to be at the TeV scale, with $\mathcal{O}(10^{-6})$ Yukawas, since the light-heavy neutrino mixing would be of the order of the ratio of light to heavy neutrino masses, that is, $\theta \sim \mathcal{O}(10^{-12})$.

An interesting variation of this scheme, which may yield observable phenomenology at colliders, is provided by the (double) inverse seesaw mechanism [6–8]. In this scenario, in addition to the three right-handed neutrinos, three left-handed SM singlets, ψ_L^i, are introduced, with a Lagrangian

$$-\mathcal{L}_\nu = y_{ij}^\nu\, \bar{\ell}_{iL}\tilde{H}N_j + \frac{1}{2}\mu_{ij}\, \overline{\psi_{iL}^c}\psi_{jL} + M_{ij}\overline{N_i}\psi_{jL} + \text{h.c.}\,, \tag{1.2}$$

where y^ν, μ and M are 3×3 complex matrices such that their entries follow the hierarchy $\mu \ll y^\nu v \ll M$. In this case the active neutrino mass matrix takes the form $m_\nu \simeq (v/\sqrt{2})^2 (y^\nu)^T (M^T)^{-1}\mu M^{-1} y^\nu$. The mixing between the light neutrino and one of the heavy states, on the other hand, is not sensitive to μ. In a simplified setting with only one generation, the mixing would just be $y^\nu v/M$. Thus, the inverse seesaw scenario clearly allows for sub-eV neutrinos masses, new degrees of freedom not far from the weak scale and still a sizable light-heavy mixing. In order to have the right-handed fermions close to the electroweak scale, the inverse seesaw scenario requires the lepton number breaking parameter (matrix) μ to be at the keV scale. Thus, the "unnatural" Yukawas are exchanged by the large hierarchy $\mu/v \sim 10^{-8}$. It can be argued that μ is naturally small in the t' Hooft sense: setting $\mu \to 0$ restores a global symmetry of the Lagrangian and therefore its renormalization group running is only multiplicative.

A completely different possibility to generate neutrino masses is given by neutrinophilic Two-Higgs-Doublet Models (ν2HDM) [9–11]. In this framework, a symmetry, say Z_2 or U(1), forces one of the Higgs doublets to couple to all SM fermions, thus being responsible for their masses, while the other Higgs couples to the lepton doublets and right-handed neutrinos. This second Higgs would acquire a vacuum expectation value (vev) around the eV scale leading to naturally small neutrino masses. However, due to the smallness of the second vev, without any explicit breaking of the aforementioned symmetry, these models are either ruled out or considerably constrained by electroweak precision data [12] and low energy flavor experiments [13].

The purpose of this work is to show how the idea of ν2HDM can be used to build a realistic, phenomenologically viable, and dynamical inverse seesaw model. This is achieved by promoting the U(1) symmetry, used in ref. [11] to avoid a Majorana mass for the right-handed neutrinos, to a local symmetry. Immediately, chiral anomalies require the presence of additional fermion content beyond the three right-handed neutrinos charged under this U(1). A minimal choice would be to double the spectrum of right-handed neutrinos, with the additional ones having opposite U(1) charges. Such minimal setup is identical to the inverse seesaw framework. In order to break this extra symmetry and give mass to neutrinos, we introduce a new scalar particle, singlet under the SM gauge group but charged under the additional U(1), in such a way that we dub our model ν2HDSM (neutrinophilic Two-Higgs-Doublet + Singlet Model), to distinguish it from the ν2HDM already considered in the literature. Other proposals for a UV completion of the inverse seesaw mechanism can be found in [14–18].

The paper is organized as follows. In section 2 we build the ν2HDSM, analyzing in detail the scalar potential of the model, the modified gauge Lagrangian and the neutrino

JHEP11(2017)004

	$\mathrm{SU}(2)_L$	$\mathrm{U}(1)_Y$	$\mathrm{U}(1)_X$
Φ_1	**2**	$\frac{1}{2}$	$\frac{1}{2}$
Φ_2	**2**	$\frac{1}{2}$	0
S	**1**	0	1
N_i^c	**1**	0	$-\frac{1}{2}$
ψ_{iL}	**1**	0	$\frac{1}{2}$

Table 1. Transformation properties of the scalar and fermion fields under $\mathrm{SU}(2)_L \times \mathrm{U}(1)_Y \times \mathrm{U}(1)_X$.

mass matrix. Section 3 is devoted to the theoretical and experimental constraints which we will consider, while we present and discuss the results in section 4 and finally conclude in section 5.

2 Neutrinophilic Two-Higgs-Doublet + Singlet Model

As explained in the Introduction, a global $\mathrm{U}(1)_X$ symmetry (under which the neutrinophilic Higgs doublet Φ_1 and the right-handed neutrinos N_i have the same charge) is introduced in ref. [11], allowing for a Yukawa interaction $\overline{\ell}_{iL}\tilde{\Phi}_1 Y^\nu_{ij} N_j$ and forbidding a $\overline{N^c_i} N_i$ Majorana mass term. In addition, it forbids the other scalar doublet, Φ_2, from coupling to neutrinos. We here promote such $\mathrm{U}(1)_X$ to a local symmetry. The first interesting fact that we notice is that the gauging of $\mathrm{U}(1)_X$ requires additional fermion content to cancel anomalies. Adopting minimality as a guide, the obvious extension of the fermion sector is to add a second set of three fermions ψ_{iL}, singlets under the SM local group but with $\mathrm{U}(1)_X$ charges opposite to N^c_i. This straightforward setup already has most of the elements of the inverse seesaw scenario — only the lepton number breaking parameter μ is missing. The μ parameter can be generated dynamically by introducing a new scalar degree of freedom, which we call S, charged only under $\mathrm{U}(1)_X$. We summarize all the charges (with the $\mathrm{U}(1)_X$ ones conventionally normalized to $\pm 1/2$) in table 1. The relevant neutrino Lagrangian is

$$-\mathcal{L}_\nu = \overline{\ell}_{iL}\tilde{\Phi}_1 Y^\nu_{ij} N_j + \frac{1}{2} S^* \overline{N^c_i} Y^N_{ij} N_j + \frac{1}{2} S^* \overline{\psi^c_{iL}} Y^\psi_{ij} \psi_{jL} + \overline{N_i} M_{ij} \psi_{jL} + \text{h.c.}\,, \tag{2.1}$$

where Y^ν, Y^N, Y^ψ and M are complex 3×3 matrices. We emphasize again that one of the consequences of gauging the $\mathrm{U}(1)_X$ symmetry is to introduce the typical particle content and the Lagrangian of the inverse seesaw mechanism (although with an additional Majorana mass term for the right-handed neutrinos N_i, which plays a minor role in the neutrino mass mechanism). Before studying the phenomenological consequences of the ν2HDSM, let us notice that there is an accidental $\mathrm{U}(1)_\ell$ symmetry in the Lagrangian, whose charges are given by

$$\mathrm{U}(1)_\ell \text{ charges} \to \{\Phi_1, \Phi_2, S, \ell_{iL}, N_i, \psi_{iL}\} = \{0, 0, 2q, q, q, q\}\ . \tag{2.2}$$

This accidental symmetry corresponds to lepton number, extended in the scalar sector only to S. Since the accidental symmetry extends also to the scalar potential, we can

JHEP11(2017)004

already predict the presence of a massless Nambu Goldstone Boson in the spectrum. This is completely analog to what happens in Majoron models [19, 20], and we have explicitly checked that the massless scalar is problematic for the model to pass constraints from Electroweak Precision Measurements and bounds on Axion-Like Particles (ALPs) [21]. Pushing forward the analogy with Majorons, we introduce an explicit breaking of the accidental lepton number symmetry [22] through a dimension 5 term in the scalar potential

$$\mathcal{L}_{sb} = -\frac{g_{\rm NP}}{\Lambda} S(\Phi_1^\dagger \Phi_2)^2 + \text{h.c.}\,, \tag{2.3}$$

where $g_{\rm NP}$ is a generic New Physics (NP) coupling and Λ the scale associated with the breaking of the accidental symmetry. We notice that, given the particle content and charges of our model, it is not possible to write down $\mathrm{U}(1)_\ell$ terms with dimension smaller than 5 involving only scalars. Moreover, the addition of explicit lepton number breaking operators could, in principle, contribute to neutrino masses. Nevertheless, the smallest $\mathrm{U}(1)_\ell$ breaking term involving fermions is given by the dimension 9 operator $(\overline{\ell_L}\tilde{\Phi}_1)(\ell_L^c\tilde{\Phi}_1)(\Phi_2^\dagger\Phi_1)^2$, and thus these contributions are expected to be negligible.

It is well known that such breaking can be expected at least at the Planck scale, but we keep open the possibility that $\Lambda \neq M_{\rm PL}$. We will come back to the value of Λ in our phenomenological analysis.

2.1 Scalar potential and scalar masses

The most general ν2HDSM potential compatible with the $\mathrm{SU}(2)_L \times \mathrm{U}(1)_Y \times \mathrm{U}(1)_X$ charges of table 1 with the addition of the only dimension 5 operator that breaks $\mathrm{U}(1)_\ell$ is the following:

$$\begin{aligned}\mathcal{V}(\Phi_1,\Phi_2,S) = {} & m_{11}^2\Phi_1^\dagger\Phi_1 + m_{22}^2\Phi_2^\dagger\Phi_2 \\ & + \frac{\lambda_1}{2}\left(\Phi_1^\dagger\Phi_1\right)^2 + \frac{\lambda_2}{2}\left(\Phi_2^\dagger\Phi_2\right)^2 + \lambda_3\left(\Phi_1^\dagger\Phi_1\right)\left(\Phi_2^\dagger\Phi_2\right) + \lambda_4\left(\Phi_1^\dagger\Phi_2\right)\left(\Phi_2^\dagger\Phi_1\right) \\ & + m_S^2|S|^2 + \frac{\lambda_s}{2}|S|^4 + \left(\lambda_{1s}\Phi_1^\dagger\Phi_1 + \lambda_{2s}\Phi_2^\dagger\Phi_2\right)|S|^2 + \left[\frac{g_{\rm NP}}{\Lambda}S(\Phi_1^\dagger\Phi_2) + \text{h.c.}\right]\,,\end{aligned} \tag{2.4}$$

whose minimization is shown in appendix A. To fix the notation, we explicitly write the scalar fields as

$$\Phi_{1,2} = \begin{pmatrix} \phi_{1,2}^+ \\ \frac{1}{\sqrt{2}}\left(v_{1,2} + \rho_{1,2} + i\eta_{1,2}\right)\end{pmatrix}, \qquad S = \frac{1}{\sqrt{2}}(v_3 + \rho_3 + i\eta_3)\,, \tag{2.5}$$

where $v_{1,2,3}$ are the corresponding vevs of $\Phi_{1,2}$ and S, the EW scale $v = \sqrt{v_1^2 + v_2^2}$ and we define $t_\beta = \tan\beta \equiv v_2/v_1$, so that $c_\beta = \cos\beta \equiv v_1/v$ and $s_\beta = \sin\beta \equiv v_2/v$. After spontaneous symmetry breaking, two charged and two neutral would-be Nambu-Goldstone bosons are absorbed by the $W^\pm$, Z and a new gauge boson X. The remaining particle spectrum consists of two charged ($H^\pm$) and four neutral scalar fields: three CP-even (h, H, s) and one CP-odd (A). The CP-odd scalar would be the massless Majoron in the absence

JHEP11(2017)004

of the explicit $\mathrm{U}(1)_\ell$ breaking term $\mathcal{L}_{sb}$ in eq. (2.3). The detailed analysis of the scalar eigenstates is presented in appendix A.

Note that Higgs measurements at the LHC require one of the CP-even eigenstates, h, to be sufficiently close to the SM-like Higgs $h_{\rm SM} = c_\beta\,\rho_1 + s_\beta\,\rho_2$. We can write the scalar mass eigenstates approximately as

$$\begin{aligned} H^\pm &= -s_\beta\,\phi_1^\pm + c_\beta\,\phi_2^\pm\,, \\ h &\simeq c_\alpha\,h_{\rm SM} - s_\alpha\,H_{\rm SM} + U_{31}\,\rho_3\,, \\ H &\simeq s_\alpha\,h_{\rm SM} + c_\alpha\,H_{\rm SM} + U_{32}\,\rho_3\,, \\ s &\simeq U_{13}\,h_{\rm SM} + U_{23}\,H_{\rm SM} + \rho_3\,, \\ A &= \frac{v_1 v_2}{\sqrt{v_1^2 v_2^2 + 4v^2 v_3^2}}\left(\frac{2v_3}{v_1}\,\eta_1 - \frac{2v_3}{v_2}\,\eta_2 + \eta_3\right)\,. \end{aligned} \tag{2.6}$$

Here, $H_{\rm SM}$ is the combination orthogonal to $h_{\rm SM}$, $c_\alpha = \cos\alpha$, $s_\alpha = \sin\alpha$ parametrize most of the mixing and U_{ij} encode the rest of the mixing matrix. The alignment limit is defined by $h = h_{\rm SM}$, which requires $s_\alpha = U_{13} = U_{31} = 0$. The corresponding masses are given by

$$\begin{aligned} m_{H^\pm}^2 &= -\frac{\lambda_4\Lambda + \sqrt{2}\,g_{\rm NP} v_3}{2\Lambda}v^2\,, \\ m_{h,H}^2 &\simeq \frac{1}{2}\left(\lambda_1 v_1^2 + \lambda_2 v_2^2 \pm \sqrt{(\lambda_1 v_1^2 - \lambda_2 v_2^2)^2 + 4\lambda_{34}^2 v_1^2 v_2^2 + \frac{8v_1^2 v_2^2}{\Lambda^2}(v_3^2 - \sqrt{2}\lambda_{34}^2 v_3\Lambda)}\right)\,, \\ m_s^2 &\simeq \lambda_s v_3^2 - \frac{g_{\rm NP}}{2\sqrt{2}\Lambda}\frac{v_1^2 v_2^2}{v_3}\,, \\ m_A^2 &= \frac{-g_{\rm NP}}{2\sqrt{2}\Lambda}\frac{(v_1^2 v_2^2 + 4v^2 v_3^2)}{v_3}\,, \end{aligned} \tag{2.7}$$

where $\lambda_{34} = \lambda_3 + \lambda_4$. Notice that we need $\lambda_4\Lambda + \sqrt{2}\,g_{\rm NP} v_3 < 0$ for electromagnetism not to be broken, and $g_{\rm NP} < 0$ to ensure a positive mass for A. In what follows, we will always assume this to be the case. In fact, as we will see later requiring $\lambda_4\Lambda + \sqrt{2}\,g_{\rm NP} v_3 < 0$ is not a problem for the stability of the potential.

2.2 Gauge Lagrangian

Let us now move to the analysis of the gauge bosons and their masses. In what follows, we will, for simplicity, assume that there is no $B_{\mu\nu}X^0_{\mu\nu}$ kinetic mixing (we call X^0_μ the gauge boson associated with $\mathrm{U}(1)_X$). The scalar kinetic terms are

$$\mathcal{L}_G = \left(D_\mu\Phi_1\right)^\dagger\left(D^\mu\Phi_1\right) + \left(D_\mu\Phi_2\right)^\dagger\left(D^\mu\Phi_2\right) + \left(D_\mu S\right)^\dagger\left(D^\mu S\right)\,, \tag{2.8}$$

with the covariant derivatives given in eq. (A.7). The masses of the charged gauge bosons are easily computed and are identical to their values in the SM. In the neutral sector, instead, we have mixing between the $\{W_\mu^3, B_\mu, X_\mu^0\}$ states, resulting in the mass matrix given in eq. (A.8). Apart from the massless photon, the Z and X boson masses are given by

$$m_{Z,X}^2 = \frac{v^2}{8}\left[g^2 + g'^2 + g_X^2\,b^2 \pm \sqrt{(g^2 + g'^2 - g_X^2\,b^2)^2 + 4(g^2 + g'^2)g_X^2\,c_\beta^4}\right]\,, \tag{2.9}$$

JHEP11(2017)004

where g, g' and g_X are, respectively, the $\mathrm{SU}(2)_L$, $\mathrm{U}(1)_Y$ and $\mathrm{U}(1)_X$ coupling constants and $b \equiv \sqrt{v_1^2 + 4v_3^2}/v$. As we will see later, the electroweak $\rho = \frac{m_W^2}{c_W^2 m_Z^2}$ parameter will generically require $g_X v_1 \ll gv$. In this limit, we find that the $Z - X$ mass squared matrix becomes

$$\mathcal{M}^2_{ZX} = \frac{1}{4}\begin{pmatrix} (g^2+g'^2)v^2 & -\sqrt{g^2+g'^2}\,g_X v_1^2 \\ -\sqrt{g^2+g'^2}\,g_X v_1^2 & g_X^2(v_1^2+4v_3^2) \end{pmatrix} \simeq \begin{pmatrix} m_Z^2 & -m_Z m_X \delta \\ -m_Z m_X \delta & m_X^2 \end{pmatrix}, \quad (2.10)$$

with the approximate masses

$$\begin{aligned} m_Z^2 &\simeq \frac{1}{4}(g^2+g'^2)\,v^2\,, \\ m_X^2 &\simeq \frac{1}{4}g_X^2(v_1^2+4v_3^2)\,, \end{aligned} \quad (2.11)$$

and the $Z - X$ mass mixing parameter δ given by

$$\delta = \frac{v_1^2}{v\sqrt{v_1^2+4v_3^2}}\,. \quad (2.12)$$

The mass eigenstates in this case follow

$$\begin{aligned} W_\mu^3 &\simeq c_W\, Z_\mu + s_W\, A_\mu + g_X\,\frac{c_\beta^2}{g} c_W^2\, X_\mu\,, \\ B_\mu &\simeq -s_W\, Z_\mu + c_W\, A_\mu - g_X\,\frac{c_\beta^2}{g} c_W s_W\, X_\mu\,, \\ X_\mu^0 &\simeq -g_X\frac{c_\beta^2}{g} c_W\, Z_\mu + X_\mu\,, \end{aligned} \quad (2.13)$$

where $c_W = \cos\theta_W$, $s_W = \sin\theta_W$ and $g_X\frac{c_\beta^2}{g}c_W = \frac{g_X v_1^2}{v^2\sqrt{g^2+g'^2}} \ll 1$ is approximately the $X - Z$ mixing, its exact expression is given in eq. (A.10). Due to this mixing with the Z, the new gauge boson will acquire chiral couplings to all SM fermions. The coupling of X to a fermion f is given by

$$g_{X\bar{f}f} = g_X\frac{v_1^2}{v^2}(I_3^f - s_W^2 Q_f), \quad (2.14)$$

where $I_3^f = 0, \pm 1/2$ and Q_f are, respectively, the isospin and electric charge of f.

2.3 The neutrino sector

Let us now go back to the consequences of eq. (2.1). As already stressed, what we have obtained is a generalization of the inverse seesaw Lagrangian, with an additional Majorana mass term for the right-handed neutrinos N_i. In the $(\nu_{iL}, N_i^c, \psi_{iL})$ basis, the 9×9 mass matrix is

$$\mathcal{M} = \begin{pmatrix} 0 & Y^\nu v_1 & 0 \\ Y^{\nu T} v_1 & Y^N v_3 & M \\ 0 & M^T & Y^\psi v_3 \end{pmatrix}. \quad (2.15)$$

Comparing with eq. (1.2), we see that we obtain $\mu = Y^\psi v_3$, with the hierarchy among the elements of the matrices $Y^N v_3, Y^\psi v_3 \ll Y^\nu v_1$ automatically satisfied if $Y^N, Y^\psi \ll Y^\nu$

JHEP11(2017)004

(assuming v_1 and v_3 of the same order). If we further assume the hierarchy $Y^\nu v_1 \ll M$, the lower right block of $\mathcal{M}$ will have eigenvalues of the order of the eigenvalues of M, allowing us to integrate out N_i and ψ_{iL}. The first terms in a M^{-1} expansion of the neutrino mass matrix are then

$$\begin{aligned} m_\nu \simeq\ & (Y^\nu v_1) M^{T^{-1}} (Y^\psi v_3) M^{-1} (Y^{\nu T} v_1) \\ & + (Y^\nu v_1) M^{T^{-1}} (Y^\psi v_3) M^{-1} (Y^N v_3) M^{T^{-1}} (Y^\psi v_3) M^{-1} (Y^{\nu T} v_1)\,, \end{aligned} \tag{2.16}$$

from which we obtain the inverse seesaw contribution (the first term) plus a small correction dependent on Y^N. Notice that the neutrino masses vanish in the $v_3 \to 0$ or $Y^\psi \to 0$ limit, but not for $Y^N \to 0$. There are many parameters in the neutrino sector which are independent from the parameters in the scalar and gauge sector, making it simple to reproduce the observed values of the neutrino oscillation parameters in relevant portions of the parameter space, as we checked explicitly. Besides, this scenario could comprise leptogenesis and a WIMP-like dark matter candidate, but we do not pursue such possibilities in this manuscript.

For simplicity, we take M to be at the TeV scale, leading to TeV heavy neutrinos. The phenomenology of our inverse seesaw scenario may differ from the usual one due to the presence of the new gauge boson and the extended scalar sector, but we do not study it in this manuscript. As a final comment regarding this subject we note that if the mass scale M is assumed to be lower, e.g., a few GeV, Z and h may, through mixing, decay to heavy neutrinos. The $Z - X$ mixing could be suppressed by having a large v_3 (see eq. (2.12)) and the $h - S$ mixing could also be suppressed by small Yukawas, so both decays can be made negligible.

3 Theoretical and experimental constraints

Let us now list and explain the constraints we will impose on the parameter space of the ν2HDSM. In the numerical analysis of section 4 these constraints will be imposed to assess the phenomenological viability of the model. For clarity, we will distinguish between theoretical and experimental constraints.

Theoretical constraints:

Perturbativity: as a simplified approach, to ensure tree level perturbativity, we only require the absolute value of all the quartic couplings to be smaller than 4π, namely

$$|\lambda_1|,\ |\lambda_2|,\ |\lambda_3|,\ |\lambda_4|,\ |\lambda_s|,\ |\lambda_{1s}|,\ |\lambda_{2s}| < 4\pi. \tag{3.1}$$

Vacuum stability: to have a potential bounded from below, the quartic couplings need to satisfy some stability conditions at tree level [23],

$$\begin{aligned} &\lambda_{1,2,s} > 0\,, && \lambda_3 > -\sqrt{\lambda_1 \lambda_2}\,, && \lambda_{34} > -\sqrt{\lambda_1 \lambda_2}\,, \\ &\lambda_{1s} > -\sqrt{\lambda_1 \lambda_s}\,, && \lambda_{2s} > -\sqrt{\lambda_2 \lambda_s}\,. \end{aligned} \tag{3.2}$$

As we already stressed, having $\lambda_4\Lambda + \sqrt{2}\, g_{\rm NP} v_3 < 0$, in order to guarantee an unbroken $\mathrm{U}(1)_{\rm em}$, is not in contradiction with a stable potential.

Local minima for the potential: to be certain that the vevs in our model are local minima of the potential, we impose all the tree level masses of eq. (2.7) to be positive.

Experimental constraints:

Electroweak Precision Measurements (EWPM): as is well known, EWPM are crucial in assessing the validity of a model. However, in our analysis we will make some simplifying assumptions which we believe will capture the essential bounds. First of all, the usual treatment in terms of oblique parameters [24] is valid only when a mass gap is present between the EW and the NP scales. As it is clear from the masses we are considering, eqs. (2.7)–(2.9), this is not the case in the ν2HDSM. In principle, a better analysis would involve an extended set of oblique parameters [25, 26]. For simplicity, we will just perform the analysis in term of the usual Peskin-Takeuchi self-energy parameters S, T and U. In addition, since we always assume the $\mathrm{U}(1)_X$ gauge coupling g_X to be small to ensure $\rho \simeq 1$ already at tree level (see eq. (2.9)), and since all the X_μ contributions to the gauge bosons vacuum polarization corrections to the EW precision observables are suppressed at least by a factor g_X^2, we will neglect such contributions. We have explicitly checked that the loops we are neglecting are small as expected. In practice, we compute the oblique parameters using a Two-Higgs-Doublet+Singlet approximation [27], imposing compatibility at 1, 2 and 3 σ with the following fitted values [28]

$$\left(S^{\rm fit}, T^{\rm fit}, U^{\rm fit}\right) = \left(0.05 \pm 0.11, 0.09 \pm 0.13, 0.01 \pm 0.11\right). \tag{3.3}$$

Higgs decays: since several neutral particles with masses smaller than half of the SM Higgs mass may exist in our model, we can have new contributions to the Higgs invisible width. To be conservative, we will take the rather aggressive bound $\mathrm{BR}(h \to \text{invisible}) \lesssim 0.13$ at 95% C.L. [29], and $\Gamma^{\rm SM}_{\rm tot} = 4.07\,\mathrm{MeV}$ as the SM Higgs total decay width [30]. The important invisible channels in our model are the following:

$\underline{h \to \mathcal{S}\mathcal{S}}$: (where $\mathcal{S} = H, s, A$), with decay rate

$$\Gamma(h \to \mathcal{S}\mathcal{S}) = \frac{|g_{h\mathcal{S}\mathcal{S}}|^2}{32\pi m_h} \sqrt{1 - \frac{4m_{\mathcal{S}}^2}{m_h^2}}\,. \tag{3.4}$$

The expressions for the $g_{h\mathcal{S}\mathcal{S}}$ couplings above are very lengthy and not much illuminating, and so we do not write them here.

$\underline{h \to XX}$: with decay width

$$\Gamma(h \to XX) = \frac{|g_{hXX}|^2}{64\pi} \frac{m_h^3}{m_X^4} \sqrt{1 - \frac{4m_X^2}{m_h^2}} \left[1 - \frac{4m_X^2}{m_h^2} + 12\frac{m_X^4}{m_h^4}\right]. \tag{3.5}$$

JHEP11(2017)004

Assuming $g_X \ll 1$ and using eqs. (A.5) and (A.6) the coupling becomes

$$g_{hXX} = \frac{g_X^2}{4v}[v_1^2 c_\alpha + v_1 v_2 s_\alpha + 4 v v_3 U_{31}]\,. \tag{3.6}$$

$\underline{h \to ZX}$: with decay width

$$\Gamma(h \to ZX) = \frac{|g_{hZX}|^2}{64\pi}\frac{[(m_h^2 - m_Z^2)^2 + m_X^2(m_X^2 + 10 m_Z^2 - 2m_h^2)]}{m_h m_X^2 m_Z^2} \times\sqrt{1 - \frac{(m_X + m_Z)^2}{m_h^2}}\sqrt{1 - \frac{(m_X - m_Z)^2}{m_h^2}} \tag{3.7}$$

where the coupling, in the limit $g_X \ll 1$, reads

$$g_{hZX} = -\frac{g g_X}{2 c_W} v_1 s_\alpha\,. \tag{3.8}$$

$\underline{h \to A\mathcal{V}}$: (where $\mathcal{V} = X, Z$), with decay rate

$$\Gamma(h \to A\mathcal{V}) = \frac{|g_{hA\mathcal{V}}|^2}{16\pi}\frac{m_h^3}{m_\mathcal{V}^2}\left[1 - \frac{(m_\mathcal{V} - m_A)^2}{m_h^2}\right]^{3/2}\left[1 - \frac{(m_\mathcal{V} + m_A)^2}{m_h^2}\right]^{3/2}, \tag{3.9}$$

and couplings

$$g_{hAX} = \frac{g_X[-U_{31} v_1 + \cos(\alpha - \beta) v_3]}{\sqrt{v_1^2 + 4 v_3^2}} \tag{3.10}$$

$$g_{hAZ} = -\frac{\sqrt{g^2 + g'^2}}{\sqrt{v_1^2 + 4 v_3^2}} v_3 s_\alpha\,. \tag{3.11}$$

In addition to the constraint on the Higgs invisible decay width, we must verify that the visible decay widths of h into SM particles are not too different from their SM values. We thus have

$\underline{h \to SM\,SM}$: where SM stands for all the SM channels measured at the LHC. According to [31], we allow for at most a 15% departure from the SM values.

Z invisible width: the decay of Z to light particles through $Z \to \mathcal{S}A$ and $Z \to X\mathcal{S}$ (where $\mathcal{S} = H, s$) can contribute to the Z invisible width. Comparing the LEP result with the SM prediction for Z to invisible, we find that $\Gamma^{\rm NP}(Z \to \text{invisible}) < 1.8\,\text{MeV}$ at 3σ [12]. The partial decay width for such processes are

$$\begin{aligned}
\Gamma(Z \to \mathcal{S}A) &= \frac{|g_{Z\mathcal{S}A}|^2}{16\pi} m_Z \left[1 - \frac{(m_\mathcal{S} - m_A)^2}{m_Z^2}\right]^{3/2}\left[1 - \frac{(m_\mathcal{S} + m_A)^2}{m_Z^2}\right]^{3/2}, \\
\Gamma(Z \to \mathcal{S}X) &= \frac{|g_{Z\mathcal{S}X}|^2}{64\pi}\frac{[(m_Z^2 - m_\mathcal{S}^2)^2 + m_X^2(m_X^2 + 10 m_Z^2 - 2m_\mathcal{S}^2)]}{m_X^2 m_Z^3} \\
&\quad\times\sqrt{1 - \frac{(m_X + m_\mathcal{S})^2}{m_Z^2}}\sqrt{1 - \frac{(m_X - m_\mathcal{S})^2}{m_\mathcal{S}^2}}\,,
\end{aligned} \tag{3.12}$$

JHEP11(2017)004

where, assuming $g_X \ll 1$ and using eqs. (A.5) and (A.6), the couplings become

$$g_{ZHA} = -\frac{g v_3 c_\alpha}{c_W \sqrt{v_1^2 + 4v_3^2}}\,, \tag{3.13}$$

$$g_{ZsA} = -\frac{g v_3 (U_{23} - c_\beta U_{13})}{c_W \sqrt{v_1^2 + 4v_3^2}}\,, \tag{3.14}$$

$$g_{ZHX} = -\frac{g g_X v_1 c_\alpha}{2c_W}\,, \tag{3.15}$$

$$g_{ZsX} = -\frac{g g_X v_1 (U_{23} - c_\beta U_{13})}{2c_W}\,. \tag{3.16}$$

Lower bound on the charged Higgs mass: the LEP II experiment has searched for the double production of charged Higgs bosons in events with center-of-mass energy from 183 GeV to 209 GeV, with a total luminosity of 2.6 fb^{-1} [32]. Since no excess was found, we have a lower bound on the charged Higgs boson mass

$$m_{H^\pm} \gtrsim 80\,\text{GeV}. \tag{3.17}$$

In principle, bounds from the LHC should also be considered. These bounds depend, however, on t_β. In contrast, the LEP bound is obtained using charged Higgses pair production via a Z boson in the s-channel, which is t_β independent. In our model, in the large t_β limit, we have $H^\pm \to \phi_1^\pm$, which does not couple to quarks, so in this case the LEP limit prevails. In the region $t_\beta \sim 1$ the LHC bounds can be stronger than the LEP limit (in particular, if the channel $H^\pm \to \ell^\pm + N$ is open, the decay is similar to the one of sleptons in the R-parity conserving MSSM, and the bound would be $m_{H^\pm} \gtrsim 300\,\text{GeV}$ [33]). Nevertheless, a dedicated analysis would be needed to compute the correct limit in this case and this is outside the scope of our paper. Moreover, as we will see in what follows, this region will be excluded by other bounds.

Bounds on the pseudoscalar mass and couplings: depending on the size of the lepton number breaking term of eq. (2.3), a light pseudoscalar may be present in the spectrum. Such A couples to electrons through its η_2 component (see eq. (2.6)), we get a coupling

$$g_{Aee} = \frac{2 v_3 m_e}{v t_\beta \sqrt{v^2 s_{2\beta}^2 + 4v_3^2}}\,. \tag{3.18}$$

For masses $m_A \lesssim 100\,\text{keV}$, stellar cooling gives a strong bound $g_{Aee} \lesssim 2.5 \times 10^{-13}$ [21]. In our case, this translates on the bound $v_3 \lesssim 10^{-5}\,\text{GeV}$. This region of parameter space is problematic because $\Gamma(h \to XX)$ becomes too large. This can be seen using eqs. (2.11) and (3.6) in eq. (3.5), from which in the alignment limit one gets $\Gamma(h \to XX) \simeq m_h^3/(64\pi v^2)$, far above the experimental limit. In order to avoid all the ALPs bounds which limit v_3, we will thus impose $m_A \gtrsim 10\,\text{GeV}$ [21].

JHEP11(2017)004

Kaon and B decays: the presence of the light gauge boson X that mixes with Z can greatly enhance the $K \to \pi +$invisible [34, 35] branching ratio via loops [36]. There are various experiments which constrain the $Z-X$ mass mixing parameter δ given in eq. (2.12) with the typical bound of $|\delta| \lesssim 10^{-3}$–$10^{-2}$ [37]. When $v_3 \ll v_1 \ll v_2$, this parameter reads $\delta \simeq v_1/v = c_\beta$. Recasting the analysis of ref. [36] onto our scenario, we find that $K \to \pi +$ invisible constrains $c_\beta \lesssim 10^{-3}$, with some mild dependence on the mass of the charged scalars. Therefore, unless the decay is not kinematically accessible (or $114\,\text{MeV} < M_X < 151\,\text{MeV}$ due to experimental cuts), kaon physics would force $v_1 \lesssim 100\,\text{MeV}$, essentially ruling out the model. Increasing v_3 suppresses the mass mixing parameter, so that in the decoupling limit, where $v_3 \to \infty$, it goes to zero and the constraint is satisfied automatically.

The $B \to KX$ process is akin to $K \to \pi X$. By performing a similar loop calculation substituting X by its associated Goldstone boson (making use of the equivalence theorem), in the limit where all quarks but the top are massless, we reach similar conclusions: unless the decay is not kinematically accessible, the $B \to K\nu\nu$ branching ratio would put a bound on $v_3 \gtrsim 10\,\text{TeV}$ or $t_\beta \ll 1$. Moreover, there is some dependence on the mass of the charged Higgs boson. In figure 2, we show the constraints for both kaon and B decays, for different values of v_3 and fixing $M_{H^\pm} = 500\,\text{GeV}$. We will see shortly that our model is viable in the range $v_3 \sim (10 \div 10^3)\,\text{GeV}$.

$b \to s$ exclusive decays: if NP beyond the SM exists in the flavor sector, flavor changing neutral current (FCNC) processes could be modified by the exchange of unknown virtual particles. The rates of the $\bar{B} \to X_s\gamma$ [38] and $B \to \ell^+\ell^-$ [39] channels, via the exchange of $H^\pm$ in a radiative penguin diagram, put constraints on $m_{H^\pm}$ and t_β in our model. In particular, these processes set the lower bound $t_\beta \gtrsim 0.8$ for $m_{H^\pm} \lesssim 600\,\text{GeV}$.

Bounds on direct X production from accelerator experiments: the coupling of X to the SM charged fermions, via $Z - X$ mixing, can be constrained by electron and proton beam-dump experiments and B-factories, similarly to what happens in the dark photon scenario [40]. Such bounds are expected to depend strongly on t_β and v_3, since these parameters control the gauge boson mixing (see eqs. (14) and (16)). At fixed target experiments X could be produced by radiation or meson decays ($\pi^0 \to \gamma X$) and subsequently decay to a e^+e^- pair that could be measured at the detector. In our model, the presence of the invisible X partial width naturally reduces the e^+e^- branching ratio to $\sim 14\%$, weakening this bound with respect to the dark photon case. At B-factories direct X production could also be achieved, via the $X - Z$ mixing, through the process $e^+e^- \to X\mu^+\mu^-$. Moreover, differently from the dark photon phenomenology, the X axial coupling to fermions can induce $\Upsilon \to \gamma X \to \gamma +$ invisibles decays [41]. Experimental data bounds this branching ratio to be below 4.5×10^{-6}.

JHEP11(2017)004

4 Analysis of our model

Let us now analyse the viability of the ν2HDSM. We start by listing the bounds that the experimental limits discussed in section 3 impose on the parameter space. First of all, requiring $m_A \gtrsim 10\,\text{GeV}$ and $m_{H^\pm} \gtrsim 80\,\text{GeV}$ in eq. (2.7) requires $g_{\text{NP}} < 0$ and $\lambda_4 - \frac{\sqrt{2}v_3}{\Lambda} \lesssim -0.21$. The last condition automatically ensures a positive charged Higgs mass, i.e. unbroken electromagnetism. As for the lepton number breaking coupling, for definitiveness we will fix it to $g_{\text{NP}} = -1$ from now on. The requirement of being close to the alignment limit can be computed rotating eq. (A.1) to the Higgs basis. The conditions read

$$\lambda_{34} \simeq \frac{\lambda_1+\lambda_2}{2} + \frac{\lambda_1-\lambda_2}{2c_{2\beta}} - \frac{\sqrt{2}g_{\text{NP}}v_3}{\Lambda}, \qquad \lambda_{1s} \simeq \lambda_{2s} \simeq -\frac{g_{\text{NP}}v^2 s_{2\beta}}{2\sqrt{2}v_3\Lambda}. \tag{4.1}$$

Moving to the Higgs and Z invisible decays, we first notice that $\Gamma(Z \to HA)$ is always larger than the experimental limit when this channel is open. We thus require to always have $m_A + m_H > m_Z$ to kinematically close the decay. The Higgs decays to scalars of eq. (3.4) are below the experimental limit when $|g_{h\mathcal{S}\mathcal{S}}| \lesssim 2.75\,\text{GeV}$. While this is always true for $\mathcal{S} = s$, when $\mathcal{S} = H$ or A this gives the bound

$$\left|\lambda_{34} \pm \frac{\sqrt{2}v_3}{\Lambda}\right| \lesssim 0.1, \tag{4.2}$$

which applies when the channels are open. On the other hand, it is simple to check that close to the alignment limit we have $\Gamma(h \to XX) \simeq \frac{m_h^3}{64\pi v^2}\frac{c_\alpha^2 v_1^4}{(v_1^2+4v_3^2)^2}$, which can be suppressed by $v_1 \ll v_3$. The same condition can also suppress the $h \to ZX$ and $Z \to HX$ decays, as can be seen from the m_X dependence in the denominator of eqs. (3.8) and (3.13), while the $h \to AX$ and $h \to AZ$ decays are always suppressed and unimportant. It should be noted that when the $h \to XX$, $h \to ZX$ and $Z \to HX$ channels are kinematically closed, which happens when $m_X > m_h/2$ and $m_H \gtrsim 30\,\text{GeV}$, the $v_1 \ll v_3$ constraint is removed and v_1 can assume larger values (as far as $t_\beta \geq 0.8$).

An immediate consequence of the requirement $v_1 \ll v_3$ is that the pseudoscalar mass in this limit is given by $m_A^2 \simeq \frac{2v^2}{\sqrt{2}}\frac{v_3}{\Lambda}$, in such a way that the requirement $m_A \gtrsim 10\,\text{GeV}$ implies $v_3/\Lambda \gtrsim 10^{-3}$. For definitiveness, in what follows we will fix $\Lambda = 10\,\text{TeV}$, although other values may be allowed.

With these constraints in mind, we can now scan over the parameter space of the model to assess if it is phenomenologically viable. To this end, we randomly generate 18 million points and impose all the bounds described in section 3. In addition, we also require the Higgs boson mass to be in the range $123\,\text{GeV} \leq m_h \leq 127\,\text{GeV}$, the Z boson mass to be within 3 σ of the LEP measured value, $m_Z = 91.1876 \pm 0.0021\,\text{GeV}$ [42] and we require to be close to the alignment limit of eq. (4.1). More precisely, we perform a linear scan over the range of the seven quartic couplings in eq. (3.1), and a logarithmic scan over t_β, v_3 and g_X in the window

$$0.8 \leq t_\beta \leq 246\,, \qquad 10\,\text{GeV} \leq v_3 \leq 1\,\text{TeV}\,, \qquad 10^{-4} \leq g_X \leq 1\,. \tag{4.3}$$

JHEP11(2017)004

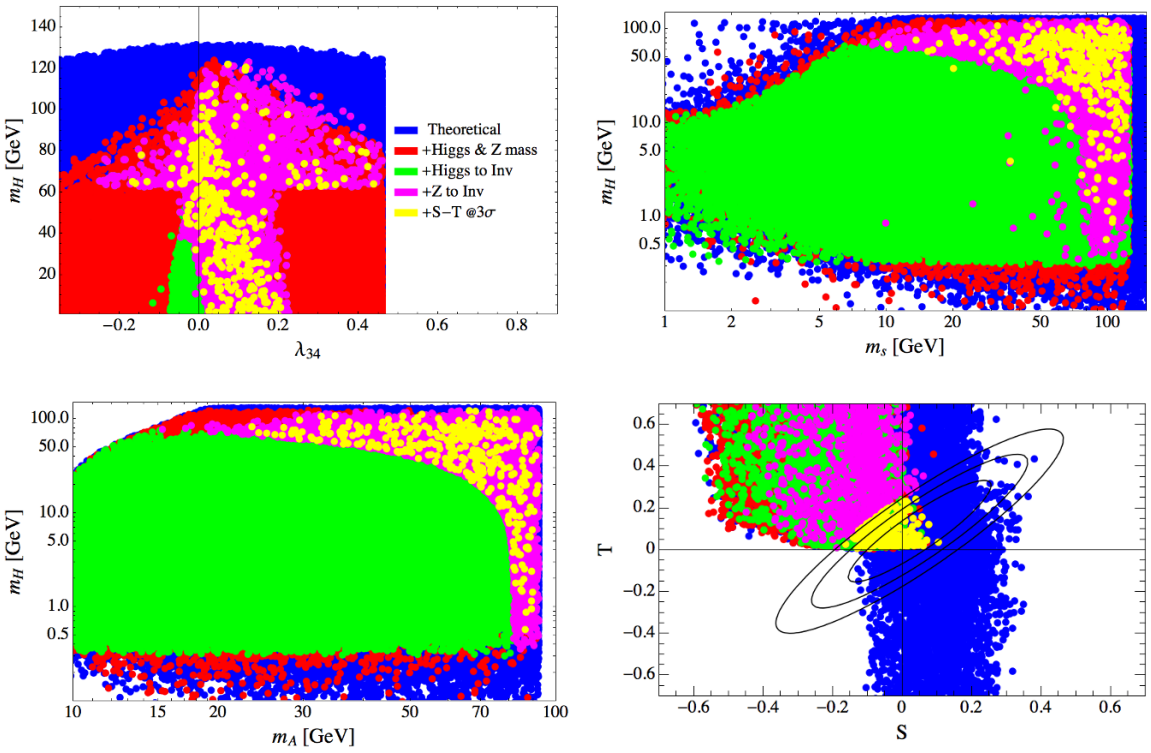

Figure 1. Effect of the theoretical and experimental constraints on the parameter space of the ν2HDSM. We show in blue the points allowed by the theoretical constraints (eqs. (3.1)–(3.2)) and $m_{H^\pm} > 80\,\text{GeV}$, in red those that also give the correct values for m_h and m_Z, in green points that in addition are allowed by $h \to$ invisible, in magenta those that also pass the limits on the Z invisible width and finally in yellow those within them that are compatible with S, T and U at 3σ. Top left: (λ_{34}, m_H). Top right: (m_s, m_H). Bottom left: (m_A, m_H). Bottom right: (S, T).

The g_X range is motivated by eq. (2.9), requiring the tree level ρ parameter to be close to 1. The lower bound on t_β is due to the $b \to s$ constraints, while we choose the upper bound (which corresponds to $v_1 = 1\,\text{GeV}$) and the v_3 range in such a way that we have $v_1 \ll v_3$ for most of the points. Using the parameters in the ranges given in eq. (4.3) we get $10\,\text{MeV} \lesssim m_X \lesssim 1\,\text{TeV}$.

The results of the scan are presented in figure 1. The color code is as follows: *(blue)*: points that pass the theoretical constraints of eqs. (3.1)–(3.2), as well as the experimental limit $m_{H^\pm} > 80\,\text{GeV}$; *(red)*: points that also give values for m_h and m_Z within the limits described above; *(green)*: points that in addition are allowed by the limits on the Higgs invisible decays (see eqs. (3.4)–(3.9)); *(magenta)*: points also allowed by the limits on the Z invisible width (see eq. (3.12)); *(yellow)*: points compatible with the EWPM limits of eq. (3.3) at 3σ.

In the upper left panel we show the different points in the (λ_{34}, m_H) plane. The preference of the experimentally allowed points for positive values of λ_{34} is due to the alignment limit of eq. (4.1), since $\lambda_{1,2}$ are always positive due to the vacuum stability constraint (see eq. (3.2)). We can now clearly see that two regions appear after imposing the bounds on $h \to$ invisible (and are maintained by the subsequent bounds). The first

JHEP11(2017)004

one corresponds to m_A, $m_H \lesssim m_h/2$, i.e. the region in which the constraint of eq. (4.2) applies. This forces λ_{34} to be below 0.25. When the $h \to HH$ and $h \to AA$ decays close, larger values of λ_{34} are allowed. In this region, the upper bound on m_H is due to the upper bound on v_1 coming from the Higgs mass in eq. (2.7).

Turning to the upper right and the lower left panels of figure 1, we have that, in addition to the bounds on m_H already discussed, a lower and an upper bound on the s and A masses appear for the experimentally allowed points. The upper bound on m_s comes from the Higgs mass constraint, while the upper bound on m_A is due to the fact that it grows with v_3 (see eq. (2.7)) and is subject to the upper bound given in eq. (4.3). The lower bound (which depends on the value of m_H and appears after the $Z \to$ invisible limit is imposed) is instead due to the requirement $m_A + m_H > m_Z$ already discussed.

Finally, we show in the right lower panel of figure 1 the points in the (S, T) plane. The dominant contribution to S and T is due to the charged scalar (whose mass, for our choice of parameters and after applying all the bounds, is in the range $80\,\text{GeV} \lesssim m_{H^\pm} \lesssim 600\,\text{GeV}$), and pushes T to positive and S to negative values. A surprising feature of the allowed points is that, somewhat counterintuitively, a light H scalar with mass $1\,\text{GeV} \lesssim m_H \lesssim 20\,\text{GeV}$ does not give a too large contribution to EWPM. This is due to the fact that we are very close to the alignment limit, with the H scalar almost completely decoupled from the Z and W gauge bosons.

Let us conclude by showing, in figure 2, the bounds on the (t_β, g_X) plane. The lower bound on t_β comes from the upper bound on $m_{H^\pm}$ obtained from exclusive $b \to s\gamma$ decays which result in excluding the region $t_\beta \lesssim 0.8$ for $m_{H^\pm} \lesssim 600\,\text{GeV}$ [38]. A milder lower bound is provided instead by the theoretical requirement of a perturbative top Yukawa coupling, eliminating $t_\beta \lesssim 0.3$. Turning to g_X, we have that upper bounds can also be set by the stipulation of having a perturbative g_X at the scale Λ and by asking for compatibility with the observed value of ρ. In particular, the cyan region is excluded by imposing $\rho - 1 = \hat{\alpha}(M_Z)T = \frac{1}{127}(0.09\text{–}0.26)$ [42]. The lower bounds are, however, more interesting. As already explained in section 3, they come from the processes $K^\pm \to \pi^\pm +$ invisible and $B^\pm \to K^\pm +$ invisible which, in our case, can be mediated by the X boson. When a model allows for an extra neutral gauge boson with mass mixing with the SM Z, these decay modes will give rise to severe experimental constraints on this mixing. In our case, after applying all the theoretical and experimental restrictions to our model, we get an upper bound on the mass mixing parameter $\delta \lesssim 0.07$ (see eq. (2.12)), a slightly larger value than the experimentally allowed one. Therefore, we need to close the aforementioned kaon and B decays and as a result, we get lower bounds on m_X and g_X. As the excluded lower regions in figure 2 show, these constraints strongly depend on the assumed value of v_3. B decays depend also on m_{H^+} and may impose a limit on t_β, on the other hand, kaon decays basically only control g_X. As in our model we have

$$\delta \sim 10^{-3} \frac{(v_1/100\,\text{GeV})^2}{v\sqrt{(v_1/100\,\text{GeV})^2 + 4\,(v_3/20\,\text{TeV})^2}}\,, \tag{4.4}$$

we see that for values of $v_1 < 100\,\text{GeV}$, the restrictions from both meson decays are lifted if $v_3 > 20\,\text{TeV}$ and hence, in this case, g_X can be as small as possible. Note that for such a large v_3 one would have to consider a much larger breaking scale Λ.

JHEP11(2017)004

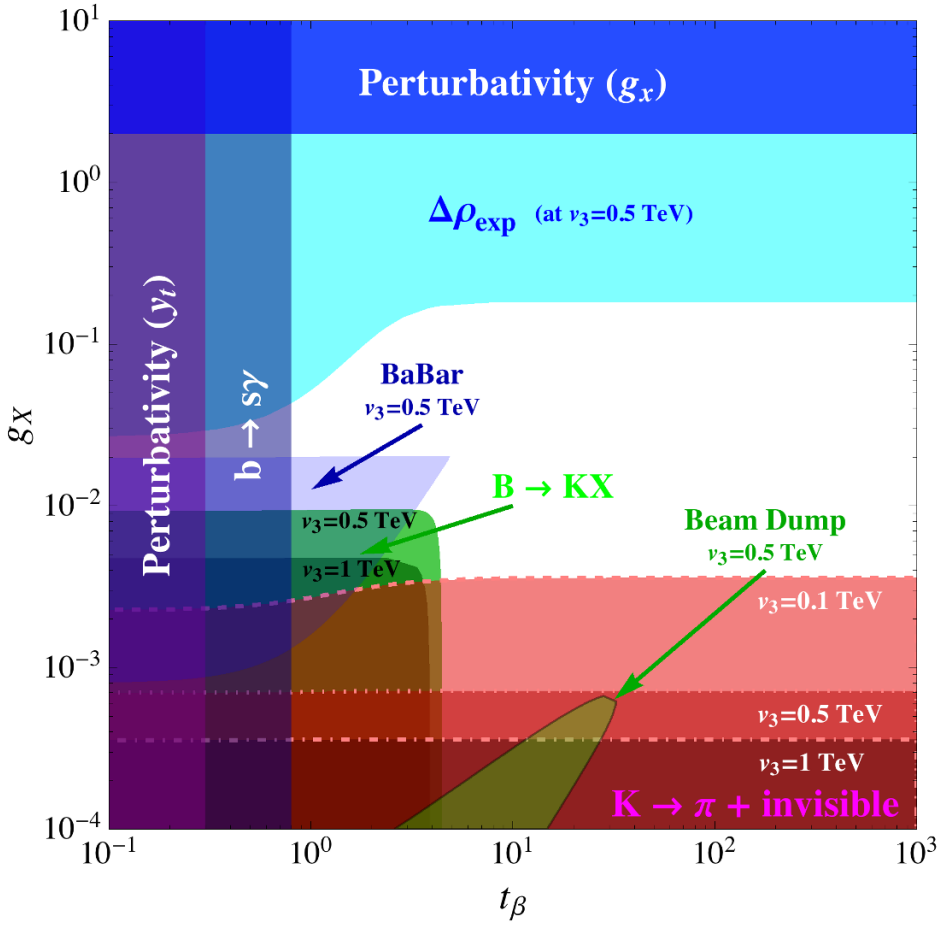

Figure 2. Bounds on the (t_β, g_X) plane coming from different theoretical and experimental sources. The colored regions are excluded.

Finally, since X can couple to the SM fermions we also get limits on $g_{Xf\bar{f}} \sim g_X c_\beta^2$ (see eq. (2.14)). The main constraint comes from beam-dump experiments (light green region) which mainly affects low masses ($m_X \lesssim 1\,\text{GeV}$) and, consequently, g_X couplings in a range already excluded by $K^\pm \to \pi^\pm +$ invisible. On the other hand, the BaBar experiment, which is sensitive to $0.02\,\text{GeV} < m_X < 10.2\,\text{GeV}$, excludes $g_{Xf\bar{f}} > 4 \times 10^{-4}$ [43] (light blue region). Since these experiments are responsive to $m_X \lesssim 10\,\text{GeV}$ the strongest constraints appear for smaller values of v_3. The limit from $\Upsilon \to \gamma X$ decay, discussed in section 3, is omitted here as it does not exclude any new region of the parameter space that is not already covered by other bounds.

5 Conclusions

The origin of neutrino masses is a long standing puzzle in particle physics. In this work, we have proposed a new realization of the inverse seesaw mechanism based on a *neutrinophilic* Two-Higgs-Doublet Model, with the $\text{U}(1)_X$ symmetry introduced to forbid a Majorana mass for the right-handed neutrinos promoted to a gauge symmetry. As we have shown, the minimal particle content that allows for a spontaneous breaking of the $\text{U}(1)_X$ and that

JHEP11(2017)004

cancels anomalies is precisely what is needed to construct an inverse seesaw model with the addition of a Majorana mass for the right-handed neutrinos. We have then focused on the viability of the model, analyzing the parameter space which is allowed by experiments. Our main results are shown in figure 1, which show the allowed values of the parameters in the scalar/gauge sector. As can be seen, the parameter space is strongly constrained by the Higgs and Z boson decays and by electroweak precision tests. Nevertheless, there is still a considerably large region where the model is perfectly viable. Some of this region may be scrutinized in the future with improvements of the h to invisible decay width measurements. In addition, $K^{\pm} \to \pi^{\pm} +$ invisible and $B^{\pm} \to K^{\pm} +$ invisible as well as dark photon searches in e^+e^- and beam dump experiments already place lower bounds on g_X, the new gauge boson coupling. Future experiments (like CERN Na62 [44] and Fermilab ORKA [45]) should be able to improve the sensitivity to these meson decays by at least one order of magnitude, testing values of g_X that would otherwise only be accessible if a future high energy lepton collider like the FCC-ee would be built. The proposed SHiP experiment at CERN [46] may also be able to extend the beam dump limits to higher values of m_X. These lower bounds on g_X, however, depend on the assumed value of v_3. In the neutrino sector we do not expect major changes with respect to what happens for the usual implementation of the (double) inverse seesaw mechanism. In contrast, what are the constraints that might be obtained by supplementary requiring a successful leptgenesis and/or the presence of a good dark matter candidate is not simple to predict. This will be analyzed in a separate publication.

Acknowledgments

This work was supported by Fundação de Amparo à Pesquisa do Estado de São Paulo (FAPESP) and Conselho Nacional de Ciência e Tecnologia (CNPq). This project has also received funding from the European Union's Horizon 2020 research and innovation programme under the Marie Sklodowska-Curie grant agreement No. 674896. This manuscript has been authored by Fermi Research Alliance, LLC under Contract No. DE-AC02-07CH11359 with the U.S. Department of Energy, Office of Science, Office of High Energy Physics. The United States Government retains and the publisher, by accepting the article for publication, acknowledges that the United States Government retains a non-exclusive, paid-up, irrevocable, world-wide license to publish or reproduce the published form of this manuscript, or allow others to do so, for United States Government purposes.

A Some detail on the scalar and gauge masses

In this appendix we present some useful detail about the diagonalization of the scalar and mass matrices. Minimizing the potential in eq. (2.4) we find that the mass matrices for the CP-even and CP-odd scalars (defined as in eq. (2.5)) are given by

$$\mathcal{M}^2_{\text{CP-even}} = \begin{pmatrix} \lambda_1 v_1^2 & \lambda_{34} v_1 v_2 + \frac{\sqrt{2} g_{\text{NP}} v_1 v_2 v_3}{\Lambda} & \lambda_{1s} v_1 v_3 + \frac{g_{\text{NP}} v_1^2 v_2}{\sqrt{2}\Lambda} \\ \lambda_{34} v_1 v_2 + \frac{\sqrt{2} g_{\text{NP}} v_1 v_2 v_3}{\Lambda} & \lambda_2 v_2^2 & \lambda_{2s} v_2 v_3 + \frac{g_{\text{NP}} v_1 v_2^2}{\sqrt{2}\Lambda} \\ \lambda_{1s} v_1 v_3 + \frac{g_{\text{NP}} v_1^2 v_2}{\sqrt{2}\Lambda} & \lambda_{2s} v_2 v_3 + \frac{g_{\text{NP}} v_1 v_2^2}{\sqrt{2}\Lambda} & -\frac{g_{\text{NP}} v_1^2 v_2^2}{2\sqrt{2}\Lambda v_3} + \lambda_s v_3^2 \end{pmatrix}, \quad \text{(A.1)}$$

and

$$\mathcal{M}^2_{\text{CP-odd}} = \frac{g_{\text{NP}}}{\Lambda}\begin{pmatrix} -\sqrt{2}v_1^2 v_3 & \sqrt{2}v_1 v_2 v_3 & -v_1^2 v_2/\sqrt{2} \\ \sqrt{2}v_1 v_2 v_3 & -\sqrt{2}v_2^2 v_3 & v_1 v_2^2/\sqrt{2} \\ -v_1^2 v_2/\sqrt{2} & v_1 v_2^2/\sqrt{2} & -\frac{v_1^2 v_2^2}{2\sqrt{2}v_3} \end{pmatrix}. \tag{A.2}$$

The CP-odd matrix is easily diagonalized; the only massive state (the *would-be Majoron* A) gets its mass via the explicit $\mathrm{U}(1)_\ell$ breaking term, and we have

$$\begin{aligned} m_A^2 &= -\frac{g_{\text{NP}}}{\Lambda}\frac{v_1^2 v_2^2 + 4v^2 v_3^2}{2\sqrt{2}v_3^2}\,, \\ A &= \frac{v_1 v_2}{\sqrt{v_1^2 v_2^2 + 4v^2 v_3^2}}\left(\frac{2v_3}{v_1}\eta_1 - \frac{2v_3}{v_2}\eta_2 + \eta_3\right). \end{aligned} \tag{A.3}$$

In order to diagonalize the CP-even squared mass matrix we instead use perturbation theory. Defining the Higgs basis according to

$$h_{\text{SM}} = \frac{v_1}{v}\rho_1 + \frac{v_2}{v}\rho_2\,, \qquad H_{\text{SM}} = -\frac{v_2}{v}\rho_1 + \frac{v_1}{v}\rho_2\,, \tag{A.4}$$

and the mass eigenbasis as

$$\begin{pmatrix} h_{\text{SM}} \\ H_{\text{SM}} \\ \rho_3 \end{pmatrix} = U \begin{pmatrix} h \\ H \\ s \end{pmatrix}, \tag{A.5}$$

we get, to first order in the perturbation parameters $\mathcal{M}_{13,23}$,

$$\begin{aligned} h &\simeq c_\alpha h_{\text{SM}} + s_\alpha H_{\text{SM}} + U_{31}\rho_3 \\ H &\simeq -s_\alpha h_{\text{SM}} + c_\alpha H_{\text{SM}} + U_{32}\rho_3 \\ s &\simeq U_{13} h_{\text{SM}} + U_{23} H_{\text{SM}} + \rho_3\,, \end{aligned} \tag{A.6}$$

where all the elements U_{ij} with either $i = 3$ or $j = 3$ are $\mathcal{O}(\mathcal{M}_{13,23})$ and c_α, s_α are the rotation elements computed diagonalizing the 2×2 block involving h_{SM} and H_{SM}. The masses computed with this approximation are presented in eq. (2.7).

Let us now turn to the gauge sector. The covariant derivatives in the scalar sector are given by

$$\begin{aligned} D_\mu \Phi_1 &= \left(\partial_\mu - i\frac{g}{2}W_\mu^i \tau^i - i\frac{g'}{2}B_\mu - i\frac{g_X}{2}X_\mu^0\right)\Phi_1, \\ D_\mu \Phi_2 &= \left(\partial_\mu - i\frac{g}{2}W_\mu^i \tau^i - i\frac{g'}{2}B_\mu\right)\Phi_2, \\ D_\mu S &= (\partial_\mu - i g_X X_\mu^0) S, \end{aligned} \tag{A.7}$$

The squared mass matrix of the neutral gauge bosons is

$$\mathcal{L}^{\text{m}}_{\text{gauge}} = \frac{1}{8}\begin{pmatrix} B_\mu & W_\mu^3 & X_\mu^0 \end{pmatrix}\begin{pmatrix} g'^2(v_1^2+v_2^2) & -gg'(v_1^2+v_2^2) & g' g_X v_1^2 \\ -gg'(v_1^2+v_2^2) & g^2(v_1^2+v_2^2) & -g g_X v_1^2 \\ g' g_X v_1^2 & -g g_X v_1^2 & g_X^2(v_1^2+v_3^2) \end{pmatrix}\begin{pmatrix} B_\mu \\ W_\mu^3 \\ X_\mu^0 \end{pmatrix}, \tag{A.8}$$

JHEP11(2017)004

which can be diagonalized in two steps. First of all, we can define the standard photon field according to

$$\begin{pmatrix} W_\mu^3 \\ B_\mu \end{pmatrix} = \begin{pmatrix} c_W & s_W \\ -s_W & c_W \end{pmatrix} \begin{pmatrix} Z_\mu^0 \\ A_\mu \end{pmatrix} . \tag{A.9}$$

At this point, we can further rotate the Z^0 and X^0 fields to go to the mass eigenbasis:

$$\begin{pmatrix} Z_\mu^0 \\ X_\mu^0 \end{pmatrix} = \begin{pmatrix} c_t & s_t \\ -s_t & c_t \end{pmatrix} \begin{pmatrix} Z_\mu \\ X_\mu \end{pmatrix} , \tag{A.10}$$

where $c_t = \cos\theta_t$ and $s_t = \sin\theta_t$, so that

$$\tan 2t = \frac{2 g_X c_\beta^2 \sqrt{g^2 + g'^2}}{g^2 + g'^2 - g_X^2 c_{\beta'}^2} . \tag{A.11}$$

The masses of the neutral gauge bosons are given in eq. (2.9), with the first order expansion for $g_X v_1 \ll g v$ given in eq. (2.11).

References

[1] Planck collaboration, P.A.R. Ade et al., *Planck 2015 results. XIII. Cosmological parameters*, *Astron. Astrophys.* **594** (2016) A13 [arXiv:1502.01589] [INSPIRE].

[2] Troitsk collaboration, V.N. Aseev et al., *An upper limit on electron antineutrino mass from Troitsk experiment*, *Phys. Rev.* **D 84** (2011) 112003 [arXiv:1108.5034] [INSPIRE].

[3] P. Minkowski, $\mu \to e\gamma$ *at a Rate of One Out of* 10^9 *Muon Decays?*, *Phys. Lett.* **B 67** (1977) 421 [INSPIRE].

[4] R.N. Mohapatra and G. Senjanović, *Neutrino Mass and Spontaneous Parity Violation*, *Phys. Rev. Lett.* **44** (1980) 912 [INSPIRE].

[5] J. Schechter and J.W.F. Valle, *Neutrino Masses in* SU(2) × U(1) *Theories*, *Phys. Rev.* **D 22** (1980) 2227 [INSPIRE].

[6] D. Wyler and L. Wolfenstein, *Massless Neutrinos in Left-Right Symmetric Models*, *Nucl. Phys.* **B 218** (1983) 205 [INSPIRE].

[7] R.N. Mohapatra and J.W.F. Valle, *Neutrino Mass and Baryon Number Nonconservation in Superstring Models*, *Phys. Rev.* **D 34** (1986) 1642 [INSPIRE].

[8] M.C. Gonzalez-Garcia and J.W.F. Valle, *Fast Decaying Neutrinos and Observable Flavor Violation in a New Class of Majoron Models*, *Phys. Lett.* **B 216** (1989) 360 [INSPIRE].

[9] S. Gabriel and S. Nandi, *A New two Higgs doublet model*, *Phys. Lett.* **B 655** (2007) 141 [hep-ph/0610253] [INSPIRE].

[10] N. Haba and K. Tsumura, *ν-Two Higgs Doublet Model and its Collider Phenomenology*, *JHEP* **06** (2011) 068 [arXiv:1105.1409] [INSPIRE].

JHEP11(2017)004

[11] S.M. Davidson and H.E. Logan, *Dirac neutrinos from a second Higgs doublet*, *Phys. Rev.* **D 80** (2009) 095008 [arXiv:0906.3335] [INSPIRE].

[12] P.A.N. Machado, Y.F. Perez-Gonzalez, O. Sumensari, Z.K. Tabrizi and R. Zukanovich Funchal, *On the Viability of Minimal Neutrinophilic Two-Higgs-Doublet Models*, *JHEP* **12** (2015) 160 [arXiv:1507.07550] [INSPIRE].

[13] E. Bertuzzo, Y.F. Perez-Gonzalez, O. Sumensari and R. Zukanovich Funchal, *Limits on Neutrinophilic Two-Higgs-Doublet Models from Flavor Physics*, *JHEP* **01** (2016) 018 [arXiv:1510.04284] [INSPIRE].

[14] A.G. Dias, C.A. de S. Pires, P.S. Rodrigues da Silva and A. Sampieri, *A Simple Realization of the Inverse Seesaw Mechanism*, *Phys. Rev.* **D 86** (2012) 035007 [arXiv:1206.2590] [INSPIRE].

[15] S.S.C. Law and K.L. McDonald, *Generalized inverse seesaw mechanisms*, *Phys. Rev.* **D 87** (2013) 113003 [arXiv:1303.4887] [INSPIRE].

[16] S. Fraser, E. Ma and O. Popov, *Scotogenic Inverse Seesaw Model of Neutrino Mass*, *Phys. Lett.* **B 737** (2014) 280 [arXiv:1408.4785] [INSPIRE].

[17] M. Aoki, N. Haba and R. Takahashi, *A model realizing inverse seesaw and resonant leptogenesis*, *Prog. Theor. Exp. Phys.* **2015** (2015) 113B03 [arXiv:1506.06946] [INSPIRE].

[18] W. Wang and Z.-L. Han, *Global* $\mathrm{U}(1)_L$ *Breaking in Neutrinophilic 2HDM: From LHC Signatures to X-Ray Line*, *Phys. Rev.* **D 94** (2016) 053015 [arXiv:1605.00239] [INSPIRE].

[19] Y. Chikashige, R.N. Mohapatra and R.D. Peccei, *Are There Real Goldstone Bosons Associated with Broken Lepton Number?*, *Phys. Lett.* **B 98** (1981) 265 [INSPIRE].

[20] G.B. Gelmini and M. Roncadelli, *Left-Handed Neutrino Mass Scale and Spontaneously Broken Lepton Number*, *Phys. Lett.* **B 99** (1981) 411 [INSPIRE].

[21] D. Cadamuro, *Cosmological limits on axions and axion-like particles*, arXiv:1210.3196 [INSPIRE].

[22] I.Z. Rothstein, K.S. Babu and D. Seckel, *Planck scale symmetry breaking and majoron physics*, *Nucl. Phys.* **B 403** (1993) 725 [hep-ph/9301213] [INSPIRE].

[23] A. Drozd, B. Grzadkowski, J.F. Gunion and Y. Jiang, *Extending two-Higgs-doublet models by a singlet scalar field — the Case for Dark Matter*, *JHEP* **11** (2014) 105 [arXiv:1408.2106] [INSPIRE].

[24] M.E. Peskin and T. Takeuchi, *Estimation of oblique electroweak corrections*, *Phys. Rev.* **D 46** (1992) 381 [INSPIRE].

[25] I. Maksymyk, C.P. Burgess and D. London, *Beyond S, T and U*, *Phys. Rev.* **D 50** (1994) 529 [hep-ph/9306267] [INSPIRE].

[26] C.P. Burgess, S. Godfrey, H. Konig, D. London and I. Maksymyk, *A Global fit to extended oblique parameters*, *Phys. Lett.* **B 326** (1994) 276 [hep-ph/9307337] [INSPIRE].

[27] W. Grimus, L. Lavoura, O.M. Ogreid and P. Osland, *The Oblique parameters in multi-Higgs-doublet models*, *Nucl. Phys.* **B 801** (2008) 81 [arXiv:0802.4353] [INSPIRE].

[28] GFITTER GROUP collaboration, M. Baak et al., *The global electroweak fit at NNLO and prospects for the LHC and ILC*, *Eur. Phys. J.* **C 74** (2014) 3046 [arXiv:1407.3792] [INSPIRE].

JHEP11(2017)004

[29] J. Ellis and T. You, *Updated Global Analysis of Higgs Couplings*, *JHEP* **06** (2013) 103 [arXiv:1303.3879] [INSPIRE].

[30] A. Denner, S. Heinemeyer, I. Puljak, D. Rebuzzi and M. Spira, *Standard Model Higgs-Boson Branching Ratios with Uncertainties*, *Eur. Phys. J.* **C 71** (2011) 1753 [arXiv:1107.5909] [INSPIRE].

[31] ATLAS and CMS collaborations, *Measurements of the Higgs boson production and decay rates and constraints on its couplings from a combined ATLAS and CMS analysis of the LHC pp collision data at* $\sqrt{s} = 7$ *and* 8 *TeV*, *JHEP* **08** (2016) 045 [arXiv:1606.02266] [INSPIRE].

[32] LEP, DELPHI, OPAL, ALEPH and L3 collaborations, G. Abbiendi et al., *Search for Charged Higgs bosons: Combined Results Using LEP Data*, *Eur. Phys. J.* **C 73** (2013) 2463 [arXiv:1301.6065] [INSPIRE].

[33] CMS collaboration, *Searches for electroweak production of charginos, neutralinos and sleptons decaying to leptons and W, Z and Higgs bosons in pp collisions at* 8 *TeV*, *Eur. Phys. J.* **C 74** (2014) 3036 [arXiv:1405.7570] [INSPIRE].

[34] E949 collaboration, V.V. Anisimovsky et al., *Improved measurement of the* $K^+ \to \pi^+ \nu\bar{\nu}$ *branching ratio*, *Phys. Rev. Lett.* **93** (2004) 031801 [hep-ex/0403036] [INSPIRE].

[35] E949 collaboration, A.V. Artamonov et al., *New measurement of the* $K^+ \to \pi^+ \nu\bar{\nu}$ *branching ratio*, *Phys. Rev. Lett.* **101** (2008) 191802 [arXiv:0808.2459] [INSPIRE].

[36] H. Davoudiasl, H.-S. Lee and W.J. Marciano, *Muon* $g-2$*, rare kaon decays and parity violation from dark bosons*, *Phys. Rev.* **D 89** (2014) 095006 [arXiv:1402.3620] [INSPIRE].

[37] H. Davoudiasl, H.-S. Lee and W.J. Marciano, *"Dark" Z implications for Parity Violation, Rare Meson Decays and Higgs Physics*, *Phys. Rev.* **D 85** (2012) 115019 [arXiv:1203.2947] [INSPIRE].

[38] M. Misiak and M. Steinhauser, *Weak radiative decays of the B meson and bounds on* $M_{H^\pm}$ *in the Two-Higgs-Doublet Model*, *Eur. Phys. J.* **C 77** (2017) 201 [arXiv:1702.04571] [INSPIRE].

[39] P. Arnan, D. Bečirević, F. Mescia and O. Sumensari, *Two Higgs Doublet Models and* $b \to s$ *exclusive decays*, arXiv:1703.03426 [INSPIRE].

[40] F. Bossi, *Dark Photon Searches Using Displaced Vertices at Low Energy* e^+e^- *Colliders*, *Adv. High Energy Phys.* **2014** (2014) 891820 [arXiv:1310.8181] [INSPIRE].

[41] K.S. Babu, A. Friedland, P.A.N. Machado and I. Mocioiu, *Flavor Gauge Models Below the Fermi Scale*, arXiv:1705.01822 [INSPIRE].

[42] Particle Data Group collaboration, C. Patrignani et al., *Review of Particle Physics*, *Chin. Phys.* **C 40** (2016) 100001 [INSPIRE].

[43] BaBar collaboration, J.P. Lees et al., *Search for a Dark Photon in* e^+e^- *Collisions at BaBar*, *Phys. Rev. Lett.* **113** (2014) 201801 [arXiv:1406.2980] [INSPIRE].

[44] G. Ruggiero for the NA62 collaboration, *The NA62 Experiment: Prospects for the* $K^+ \to \pi^+ \nu\bar{\nu}$ *Measurement*, PoS(KAON13)032 [INSPIRE].

[45] ORKA collaboration, E.T. Worcester, *ORKA: The Golden Kaon Experiment*, *Nucl. Phys. Proc. Suppl.* **233** (2012) 285 [arXiv:1211.4883] [INSPIRE].

[46] W.M. Bonivento, *The SHiP experiment at CERN*, *J. Phys. Conf. Ser.* **878** (2017) 012014 [INSPIRE].

JHEP11(2017)004